

Observation of abruptly autofocusing waves

Dimitrios G. Papazoglou,^{1,2,5} Nikolaos K. Efremidis,³ Demetrios N. Christodoulides,⁴ and Stelios Tzortzakis^{1,6}

¹*Institute of Electronic Structure and Laser, Foundation for Research and Technology Hellas, P.O. Box 1527, 71110, Heraklion, Greece*

²*Materials Science and Technology Department, University of Crete, P.O. Box 2208, 71003, Heraklion, Greece*

³*Applied Mathematics Department, University of Crete, P.O. Box 2208, 71003, Heraklion, Greece*

⁴*CREOL/College of Optics, University of Central Florida, Orlando, Florida 32816, USA*

⁵*e-mail: dpapa@materials.uoc.gr*

⁶*e-mail: stzortz@iesl.forth.gr*

Received February 25, 2011; revised March 31, 2011; accepted April 13, 2011;
posted April 18, 2011 (Doc. ID 143297); published May 9, 2011

We report on the experimental observation of abruptly autofocusing waves. This interesting family of wave packets has been realized by using a radially symmetric Airy intensity distribution. As demonstrated in our experiments, these waves can exhibit unusual features, such as the ability to autofocus by following a parabolic trajectory toward their focus. © 2011 Optical Society of America

OCIS codes: 050.1940, 260.2030, 350.5500, 320.0320.

Optical waves are often used as a means of energy delivery on a remote target. In many applications, a Gaussian or top-hat beam is focused on a remote target by the use of a focusing element that reshapes the beam's wavefront. The main drawback of this approach is the gradual increase in the peak intensity as the focus is approached. In this case, the beam energy is delivered in an extended volume that is, in general, proportional to $V_F \propto \lambda^3 (\#F)^4$, where λ is the wavelength, $\#F$ denotes the f -number ($\#F \equiv f/D$), f is the focal distance, and D is the initial transverse size of the beam. This delivery of distributed energy is drastically enhanced as the focal length is increased. A common method to overcome this problem is to increase the initial transverse size of the beam and, consequently, of the focusing optical element. Although this is viable for short focal length microscope objectives, it is impractical for optical systems with long focal lengths, as typically used in medical applications, where typically $\#F \geq 5$.

Ideally, the problem can be resolved by inducing an asymmetry in the longitudinal intensity profile so that the energy is abruptly delivered to the focus while it maintains a low intensity up to that point. Recently, a new family of abruptly autofocusing waves was theoretically proposed [1]. These waves exhibit interesting focusing characteristics since, close to the focal point, they undergo an abrupt increase in their intensity. Because of the nature of these waves, the caustic of the intensity maxima converges in a nonlinear fashion toward the focus. In the case of a radially symmetric Airy intensity distribution, the intensity maxima follow a parabolic trajectory [1,2].

In this Letter, we demonstrate the first, to our knowledge, experimental realization of abruptly autofocusing waves using a radially symmetric Airy intensity distribution. We demonstrate that these waves autofocus, with the intensity maxima following a parabolic trajectory. The intensity contrast achieved is much higher than that of a typical Gaussian beam, making these waves interesting candidates for a variety of applications, as in bio-medicine and laser nanosurgery.

The radially symmetric Airy distribution [1] is described by

$$u_o(r, 0) = \text{Ai}\left(\frac{r_o - r}{w}\right) \exp\left[a \cdot \left(\frac{r_o - r}{w}\right)\right], \quad (1)$$

where $\text{Ai}(\cdot)$ denotes the Airy function [1,2], r is the radius, r_o is the radius of the primary ring, w is a scaling factor, and a is an exponential decay factor. The radius of the highest intensity Airy ring is then $R(0) \cong (r_o - w)$, while its FWHM is $\cong 2.28w$.

The direct generation of the radially symmetric Airy distribution is not a trivial task, since combined phase and amplitude modulation are required. Alternatively, such a distribution can be generated through the Fourier transform (FT) of a properly modulated input wave. This approach was successfully applied in generating one-dimensional (1D) and two-dimensional (2D) Airy beams [2–4]. In this latter case, the FT is a Gaussian beam modulated by a cubic phase so only phase modulation is required. On the other hand, the FT of the radially symmetric Airy distribution, which cannot be described by a simple analytical form, is a Bessel-like distribution with a central peak surrounded by decaying amplitude rings [1]. Although this distribution changes signs as a function of the radius, it can be generated by encoding both amplitude and phase information onto a phase-only filter using a technique proposed by Davis *et al.* [5]. This versatile technique is based on the idea that the phase modulation of a diffracting phase element leads to a spatial modulation of its diffraction efficiency so that energy is selectively transferred between the diffraction orders, more specifically, the zero and first orders, allowing the modulation of their amplitude.

In our case, the FT of the radially symmetric Airy distribution is firstly encoded onto a phase filter, which is applied onto a phase-only reflecting spatial light modulator (SLM) screen (Hamamatsu LCOS-X10468-2), as shown in Fig. 1. The phase modulation capability of this device is up to $\sim 2\pi$ therefore phase wrapping is used to implement higher phase modulation. The phase modulated reflected wavefront is then Fourier transformed

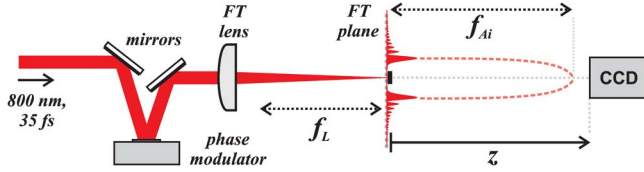


Fig. 1. (Color online) Experimental setup. FT, Fourier transform; f_L , FT lens focal length; f_{Ai} , effective focal length of the Airy ring.

by a lens ($f_L = 500$ mm). An opaque mask is used to block the undesired zero-order peak. Finally, the intensity distribution along the propagation is recorded using a linear CCD camera (12 bits, 1224×968 pixels). In our experiments, we used 1 mJ, 35 fs laser pulses at 800 nm, with a Gaussian in space and time distribution, produced by a 50 Hz, Ti:sapphire laser system. Let us now describe in more detail the procedure we followed to generate the phase-only filter. First, the FT $F_T\{u_o(\sqrt{x^2 + y^2}, 0)\} \equiv A(x, y) \exp[i\Phi(x, y)]$ of the Airy ring distribution is numerically calculated. Then, in order to compensate distortions in the encoding process, the amplitude $A(x, y)$ is slightly distorted using a lookup table [5]. Finally, the distorted amplitude is multiplied with the phase $\Phi(x, y)$ of the calculated FT [5] to generate the desired phase-only function $\Psi(x, y) = \exp[iA(x, y)\Phi(x, y)]$. The calculated phase distribution is shown in Fig. 2(a), with the corresponding 2D phase mask shown as an inset. The numerically calculated intensity profile at the FT plane is shown in Fig. 2(b). Except from the high intensity zero-order peak, the Airy ring distribution is clearly distinguishable. In our case, the energy contained in the Airy ring beam is of the order of a few microjoules, enough for the ignition of nonlinear effects in transparent media, as we will show below.

Beyond the use of SLMs, one may, as well, use specially designed amplitude/phase masks that can be used for the generation of such abruptly autofocusing waves containing even higher energies.

A typical intensity profile as captured by the CCD sensor at a distance $z = 200$ mm from the FT plane is shown in Fig. 2(c). The concentric rings of Airy ring distribution are clearly visible, accompanied by some low-intensity diffraction rings in the periphery. A proof that this is indeed a radially symmetric Airy distribution is the demonstration of its autofocusing nature.

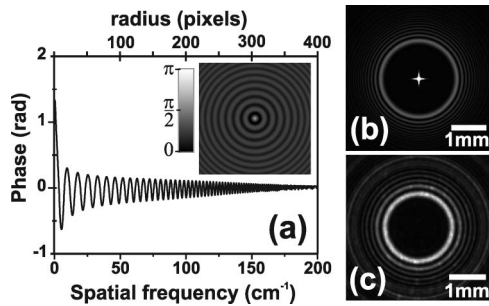


Fig. 2. (Color online) (a) Radial profile of the phase mask. Inset, phase mask (b) Theoretical intensity at the FT plane (in the center is the zero order) (c) Experimental intensity profile of the generated Airy ring as captured by the CCD at $z = 200$ mm (zero order blocked).

The intensity contrast, defined as the ratio of the peak intensity along the propagation to the peak intensity at the Fourier plane $I(z)/I(0)$ is shown in Fig. 3. As expected [1], the intensity peak follows a curved trajectory as the wave propagates toward the focus. Furthermore, the intensity contrast is abruptly increased at the focus. It is interesting to note here that the autofocusing is an inherent property of the wave. We can define an effective focal distance f_{Ai} as the distance between the plane of generation of the Airy ring (in our case, the FT plane of the lens) and the focus position. In our case, $f_{Ai} \cong 380$ mm. This distance is controlled by the initial size of the primary Airy ring and the width of the Airy intensity lobes. Using the prediction of the 1D Airy beams [2,6], the radius $R(z)$ of the primary Airy ring is described by

$$R(z) \cong (r_o - w) - 3.15 \cdot 10^{-3} (\lambda^2/w^3) \cdot z^2, \quad (2)$$

where λ is the wavelength and z is the propagation distance. By using Eq. (2), we can estimate the effective focal distance f_{Ai} (Fig. 1) of the autofocusing Airy ring as

$$f_{Ai} \cong 17.9(w^2/\lambda) \sqrt{(r_o/w - 1)}. \quad (3)$$

From Eq. (3), it is clear that the effective focus of such a wave is controlled by w and r_o . By using Eqs. (2) and (3), we can describe the radius of the primary Airy ring as a function of the initial radius $R(0)$ and the effective focal length f_{Ai} :

$$R(z) \cong R(0)(1 - z^2/f_{Ai}^2). \quad (4)$$

Figure 4(a) shows the intensity contrast as a function of the propagation distance of the generated Airy ring in comparison to an equivalent (theoretically calculated) Gaussian beam that is focused using a lens of focal distance $f = f_{Ai}$ (380 mm).

The intensity distribution of this equivalent Gaussian beam is selected to be either the envelope of the Airy ring intensity distribution (initial waist of $1893 \mu\text{m}$; referred as the equivalent envelope) or to reach the same value of peak contrast at the focus (initial waist of $2778 \mu\text{m}$; referred to as equivalent peak contrast). In this figure, we can clearly see the abruptness of the autofocusing wave compared to that of a Gaussian beam and the asymmetry along the propagation direction. The intensity contrast of the autofocusing wave is very low before the focus, while it reaches up to ~ 195 at the focus. The radius of the primary Airy ring as a function of the propagation distance is shown in Fig. 4(b). The theoretical prediction

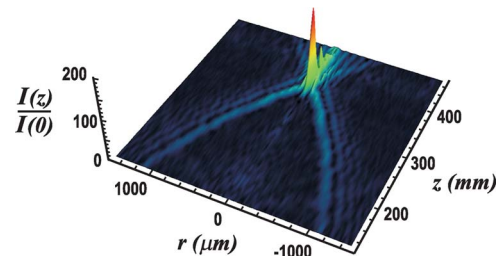


Fig. 3. (Color online) Radially averaged intensity as a function of the propagation distance. Intensity values are normalized to the peak intensity at $z = 0$.

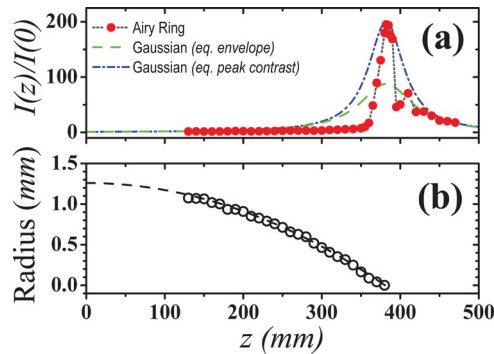


Fig. 4. (Color online) (a) Intensity contrast as a function of the propagation distance: solid circles, experimental values; dashed curve and dashed-dotted curve, intensity contrast of equivalent Gaussian beams. (b) Radius of the ring Airy as a function of the propagation distance: open circles, experimental points; dashed curve, quadratic fit.

$R(z) \cong 1260 \mu\text{m} - (8.7 \cdot 10^{-3} \mu\text{m}/\text{mm}^2) \cdot z^2$ of Eq. (2) nicely fits the experimental points, confirming that the radius shrinks in a quadratic fashion. This parabolic trajectory leads to another advantage. By using Eq. (4) to estimate the slope of the caustic near the focus, we define an effective f -number: $(\#F)_{\text{Ai}} \cong f_{\text{Ai}}/4R(0)$. This value is 2 times smaller than the f -number of a Gaussian beam with initial waist $w_G = R(0)$. Thus, to generate similarly sized focal spots, the waist of the equivalent Gaussian beam should be $w_G \cong 2R(0)$. A graphical representation of the clear advantage of the autofocusing waves in laser processing of thick samples is shown in Fig. 5(a). It is obvious that, by using these beams, a long working distance can be combined with a short focal volume, thanks to the abrupt increase of the intensity of the Airy ring at the focus. Thus, these beams are great candidates for biomedical applications and nanosurgery. As a simple example of the power of this approach, we show in Fig. 5(b) an ablation spot produced in the back side of a thick (10 mm) fused silica window using our intense Airy ring beam.

The unique characteristics of these autofocusing waves can be further enhanced by properly engineering their profile. Figure 6 shows some typical examples of this approach where the temporal profile is altered while, in the spatial domain, the distribution is always an autofocusing radially symmetric Airy beam.

As a reference, in Fig. 6(a) is shown the iso-intensity profile of a wave packet whose temporal profile is described by a Gaussian distribution. This is the type of wave packet that is used in all the experimental results in this Letter. A drawback of this temporal profile is that, in a dispersing medium, the pulse is broadened. Thus, the peak intensity and, consequently, the contrast are affected. This is not a problem for the wave packet shown in Fig. 6(b), where the temporal profile is now described by an Airy function. Since this wave is known to be non-dispersing [4,7], the high contrast will be preserved in dispersing media. Finally, the intensity contrast can be further enhanced by using the complex wave packet shown in Fig. 6(c). In this case, the temporal profile is described by two facing Airy functions, which can be seen as a 1D equivalent of the radially symmetric Airy ring distribution. In this case, beyond the nondispersive

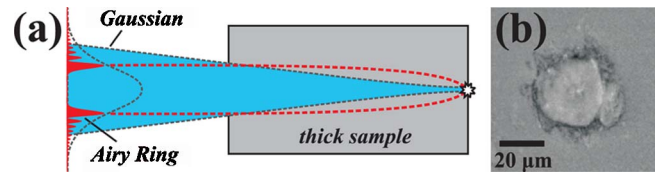


Fig. 5. (Color online) (a) Processing of a thick sample. Comparison of an Airy ring with a Gaussian beam of similar spot size. (b) Ablation crater in the back side of a 1 cm thick fused silica sample after illumination by an intense Airy ring beam.

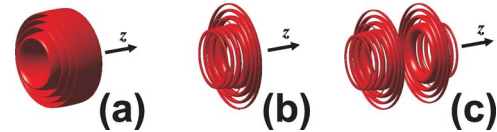


Fig. 6. (Color online) Spatiotemporal iso-intensity surface profiles of autofocusing Airy ring wave packets for various temporal profiles. (a) Gaussian temporal profile; (b) Airy temporal profile; (c) two counteraccelerating Airy temporal profiles.

character of the temporal Airy, the wave packet can be appropriately engineered so that the two counteraccelerating Airy pulses temporally collapse at the spatial focus. According to our calculations, this can further enhance the intensity contrast at the focus by (at least) a factor of 2, reaching values of ~ 400 .

In summary, we have experimentally demonstrated the generation of a novel class of abruptly autofocusing wave packets in the form of radially symmetric Airy optical beams. Compared to typical Gaussian beams, these waves exhibit enhanced contrast. Furthermore, the longitudinal intensity profile at the focus area is strongly non-symmetric, a characteristic that can be very useful for imaging and biomedical nanosurgery applications. In addition to their spatial profile, the temporal profile of these beams can be engineered to drastically enhance the intensity contrast at the focus.

This work was supported by the European Union (EU) Marie Curie Excellence Grant “MULTIRAD” MEXT-CT-2006-042683. N. K. Efremidis was partially supported by the FP7-REGPOT-2009-1 project “Archimedes Center for Modeling, Analysis and Computation” and D. N. Christodoulides by the United States Air Force Office of Scientific Research (USAFOSR) grant no. FA9550-10-1-0561.

References

1. N. K. Efremidis and D. N. Christodoulides, *Opt. Lett.* **35**, 4045 (2010).
2. G. A. Siviloglou and D. N. Christodoulides, *Opt. Lett.* **32**, 979 (2007).
3. P. Polynkin, M. Kolesik, A. Roberts, D. Faccio, P. Di Trapani, and J. Moloney, *Opt. Express* **16**, 15733 (2008).
4. D. Abdollahpour, S. Suntsov, D. G. Papazoglou, and S. Tzortzakis, *Phys. Rev. Lett.* **105**, 253901 (2010).
5. J. A. Davis, D. M. Cottrell, J. Campos, M. J. Yzuel, and I. Moreno, *Appl. Opt.* **38**, 5004 (1999).
6. P. Polynkin, M. Kolesik, J. V. Moloney, G. A. Siviloglou, and D. N. Christodoulides, *Science* **324**, 229 (2009).
7. A. Chong, W. H. Renninger, D. N. Christodoulides, and F. W. Wise, *Nat. Photon.* **4**, 103 (2010).